



# A Simulation Approach to Study the Effect of SiC Polytypism Factor on Sensitivity of Piezoresistive MEMS Pressure Sensor

Mahesh Kumar Patankar<sup>1</sup> · M. Kasinathan<sup>1</sup> · R. P. Behera<sup>1</sup> · T. Jayanthi<sup>1</sup> · Sandip Dhara<sup>2</sup>

Received: 16 November 2020 / Accepted: 16 March 2021 / Published online: 17 April 2021  
© Springer Nature B.V. 2021

## Abstract

SiC is a well known wide band gap semiconductor explored for realizing the piezoresistive micro-electro-mechanical systems (MEMS) pressure sensors for harsh environments. In this work a thin SiC diaphragm based piezoresistive pressure sensor was designed by locating the resistors of different SiC polytypes such as 3C, 4H, and 6H-SiC, on highly stressed zone of the diaphragm and analyzed. The sensor design parameters were extensively studied by executing the finite element method (FEM) and piezoresistive simulation using device simulation software. The sensor characteristics were measured for different SiC polytypes and compared for different design parameter variations to obtain the optimum sensor performance under the influence of the pressure upto 8 MPa. Influence of temperature for heavily doped SiC polytypes is also studied. The simulation results shows that the pressure sensor with 3C-SiC polytype offers higher sensitivity  $7.3 \mu\text{V/V/KPa}$  as compared to 4H-SiC and 6H-SiC polytypes.

**Keywords** MEMS · Piezoresistivity · Polytypes · SiC diaphragm · Hexagonal · Isotropic

## 1 Introduction

With the continuous increase in demand of high temperature electronics and sensors for harsh environments, scientific community concentrated the research and development on large band gap materials such as SiC, GaN, diamond [1–3] over the Si. In the case of Si, operation at increased temperature leads to high leakage current above  $150^\circ\text{C}$  [1], and high energetic radiation creates more defects which in turn device fails [4]. As a semiconductor material, SiC is getting wide acceptance because of extraordinary developments in wafer growth technology, material deposition and etching process, [5] and continuous decrease in the cost per wafer and maturing the SiC micro-electro-mechanical systems (MEMS) technology. In the recent years, SiC is positioned as a prominent

candidate in sensing applications for harsh environments due to its remarkable, extraordinary material properties such as radiation resistance, higher thermal conductivity, low intrinsic carrier concentration, chemical inertness [4]. SiC is being used in terms of mechanical sensors in different fields such as space, oil drilling, nuclear, military applications [6–8]. SiC is not only suitable for creating the MEMS structure for sensing applications but has also been used as a coating layer to protect the sensor in the corrosive environment [9].

SiC, due to the proximity of Si and C on the periodic table, is a highly covalent material that forms tetrahedral which is centered around either C or Si atoms [1]. The unique feature of SiC is that it exists in a large number of different crystallographic structures, which are called polytypes, built from the same Si-C subunit organized into a variety of stacking sequences [5]. These polytypes are described by the type of the crystal lattice i.e. hexagonal, cubic, or rhombohedral and the number of layers making up the repeat pattern [5]. There are more than 200 polytypes broadly classified into  $\alpha$ -SiC formed at a temperature greater than  $1700^\circ\text{C}$  and has a hexagonal crystal structure (similar to Wurtzite) and  $\beta$ -SiC, with a zinc blende crystal structure (similar to diamond), is formed at a temperature below  $1700^\circ\text{C}$  [10, 11]. The most common polytypes of SiC are 3C-SiC, 4H-SiC and 6H-SiC which are extensively investigated by the researchers [12].

✉ Mahesh Kumar Patankar  
patankar@igcar.gov.in

<sup>1</sup> Real Time Systems Division, Indira Gandhi Centre for Atomic Research, Homi Bhabha National Institute, Kalpakkam, Tamil Nadu 603102, India

<sup>2</sup> Surface and Nanoscience Division, Indira Gandhi Centre for Atomic Research, Homi Bhabha National Institute, Kalpakkam, Tamil Nadu 603102, India

The 3C-SiC is the only single  $\beta$ -SiC phase, whereas 4H-SiC and 6H-SiC belong to  $\alpha$ -SiC phase [12] and these polytypes can be grown on the bulk SiC substrate [13, 14].

To understand the piezoresistive phenomenon in different SiC polytypes, numerous studies have been dedicated. Basically, SiC is an anisotropic material and its piezoresistive coefficient depends on the crystallographic orientation of the material. Phan et al. [15] characterized the orientation dependence of *p*-type 3C-SiC. However, the interesting fact about hexagonal lattice is that the piezoresistive coefficients on the sides of (0001) plane for 4H-SiC and 6H-SiC are isotropic [4, 16]. The isotropic nature is more favourable for the design and fabrication of the sensors.

The piezoresistive effect is one of the most significant and widely used pressure sensing mechanism used for developing MEMS sensors as compared to other physical effects such as capacitive, optical fibre, and others. This sensing effect has been extensively used to detect mechanical signals such as pressure, force, inertia, acceleration, deflection, stress, among others enabling the miniaturization, and integration capabilities of MEMS devices with low power requirements, and simple readout circuits [17]. The different materials such as Si, carbon nanotubes, SiC, Si nanowires, diamond etc. are extensively used as piezoresistive sensing elements for realizing the pressure sensors [4, 17–20]. Si is being widely used since the discovery of the piezoresistive effect and greatly benefited by mature fabrication technologies. However, Si is not a promising candidate for high temperature applications because of its relatively low energy gap 1.12 eV and plastic formation at elevated temperature [4]. The emergence of SiC as a piezoresistive element in the semiconductor domain solves this issue because of its wide band gap, low coefficient of thermal expansion and chemical tolerance [4, 21]. In addition, SiC offers high young modulus, and high carrier mobility which makes it more attractive material to design and fabricate the electronic devices and sensors to survive in high temperature and the chemical environment without degrading their performance.

All polytypes of SiC shows the piezoresistive effect. Many researchers used 3C-SiC in form of the thin film grown on Si substrate by anisotropic etching of Si in KOH solution and the piezoresistors by reactive ion etching of SiC [22]. Generally, 4H as epilayer form on SiC substrate is commercially available [23]. The other polytype of 6H as epilayer, grown on SiC substrate, is reported to be used as the pressure sensor. There are also reports [24–26] for the growth of 3C-SiC on hexagonal SiC substrate which, however, is yet to be demonstrated for sensor applications and they are also not available commercially, to the best of our knowledge. These reports motivate to compare the effect of SiC polytypism when SiC diaphragm is created using the bulk SiC substrate and different polytypes of SiC are considered as epilayer to compare the sensitivity of the pressure sensor.

This article investigates the piezoresistive MEMS pressure sensor composed of a square size SiC diaphragm and SiC polytype based piezoresistors. SiC polytypes such as 3C-SiC, 4H-SiC and 6H-SiC were used as the piezoresistive sensing elements and were placed on the top surface of the diaphragm at the highly concentrated stressed zone to maximize the sensitivity of the pressure sensor. The physical dimension of the diaphragm was designed using the bulk SiC substrate and optimized for different parameters such as geometry, side length, thickness, diaphragm deformation and mechanical stress by executing the extensive finite element method (FEM) simulation under the influence of uniform applied pressure up to 8 MPa. The pressure sensor modeling and simulation was performed using the device simulation software to calculate the effect of SiC polytypes on the sensitivity of the pressure sensor by varying the doping concentration, bias voltage and resistor thickness. The simulation results were analyzed and compared for all the common SiC polytypes which indicated that the proposed pressure sensor structure could be used for all SiC polytypes for the fabrication of piezoresistive pressure sensor for harsh environments.

## 2 Sensor Design Theory

The piezoresistivity effect is established as the main transduction mechanism for pressure sensing applications to measure the pressure by recording the change in electrical resistance. A diaphragm based pressure sensor is simple in design. The key mechanical structure of a diaphragm based pressure sensor is a flexible thin diaphragm and deflects under the influence of the pressure diaphragm. In addition to deflection, the other parameter of the diaphragm is mechanical stress which is felt on the application of the pressure. The other key sensing element is piezoresistors. In the presence of external pressure leads to a change in resistivity of the sensing elements accordingly [4]. The basic structure of the piezoresistive pressure sensor is shown in Fig. 1. In the following sections, mathematical analysis is carried out for flexible diaphragm followed by piezoresistor on the application of pressure sensor.

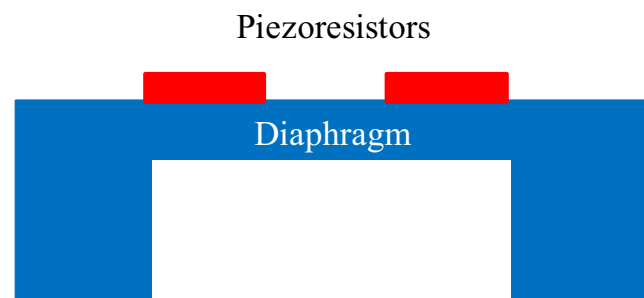


**Fig. 1** The schematic of basic piezoresistive MEMS pressure sensor structure

### 2.1 Mathematical Analysis of Thin Diaphragm

The diaphragm can be made of different possible geometries and among them, square, circular and rectangular are more common. The square size diaphragm is considered over other rest of the geometries because it offers maximum mechanical stress, and therefore, maximum mechanical sensitivity can be obtained over diaphragms of other geometries with the same plane area [27]. Additionally, from the fabrication point of view, it is easy to dice the square diaphragm from the standard SiC wafers.

Mathematically, it is very much important to first quantify the mechanical stress and the deflection in the diaphragm with pressure. Elastic deflection of diaphragm is considered for the calculation where the diaphragm is taken as a plate and its deflection depends upon its material properties, geometric configuration and boundary conditions, and on the magnitude of the loading for which it is suspended. The common method for the analysis of suspended diaphragm as a function of pressure is to adopt load-deflection method provided as the pressure-deflection relationship of a flat square diaphragm clamped at all four sides and is represented by the following equation [28]:

$$\frac{Pa^4}{Yh^4} = \frac{66.2}{(1-\nu^2)} \left(\frac{y}{h}\right) + \frac{31.1}{(1-\nu^2)} \left(\frac{y}{h}\right)^3 \tag{1}$$

where  $P$  is applied pressure,  $Y$  is Young’s modulus,  $\nu$  is Poisson’s ratio of the diaphragm material,  $a$  is the side length of the diaphragm,  $h$  is the diaphragm thickness, and  $y$  is the centre deflection of the diaphragm.

The two terms related to  $y/h$  and the second term related to  $(y/h)^3$  present in Eq. (1). The significant observation is that the small deflection theory is considered when the diaphragm deflects 1/5 times the diaphragm thickness, otherwise a large deflection theory can be adopted for diaphragm analysis. To maintain the linearity between applied pressure and stress it is obvious that the diaphragm must deflect at the center and the deflection must be less than the quarter thickness of the diaphragm. Thus, to understand the mechanical performance of the square diaphragm, the first term of Eq. (1) is given below is considered under the uniform load:

$$y = \frac{Pa^4(1-\nu^2)}{66.2 Yh^3} \tag{2}$$

Mechanical stress is another crucial factor which determines the dimension of the diaphragm hence it is required to establish the linear relation between the applied pressure and the mechanical stress. The maximum stress  $\sigma_{max}$  occurs in the middle of the diaphragm edges, and is calculated by using the following Eq. (3) [28]:

$$\sigma_{max} = 0.3078 \frac{Pa^2}{h^2} \tag{3}$$

In square diaphragm, the symmetric stress component in  $xx$  and  $yy$  directions are calculated by using the following equation:

$$(\sigma_{xx})_{max} = (\sigma_{yy})_{max} = 0.3078 \frac{Pa^2}{h^2} \tag{4}$$

where  $\sigma_{xx}$  and  $\sigma_{yy}$  are mechanical stress components in  $xx$  and  $yy$  directions, respectively.

For designing the square shaped SiC diaphragm mechanical properties:  $Y=448$  GPa,  $\nu=0.21$  and material density =  $3.3 \text{ g/cm}^3$  were considered [4]. The side length of the square diaphragm was optimized at  $1500 \text{ }\mu\text{m}$  whereas its thickness at  $50 \text{ }\mu\text{m}$  to measure the pressure upto  $8 \text{ MPa}$  (Table 1).

### 2.2 Mathematical Analysis of Piezoresistors

The next important sensing element of the pressure sensor is piezoresistors. The mechanical stress due to pressure change the resistivity of the piezoresistors. The relative change of resistivity is greatly influenced by the applied stress ( $\sigma$ ) and can also be presented as a function of the applied stress, and piezoresistive coefficient.

The piezoresistance properties of SiC material were quantified using piezoresistance coefficients,  $\pi$ , which relate the change in piezoresistivity to stress and are expressed in  $\text{Pa}^{-1}$  [21]:

$$\frac{\Delta\rho}{\rho} = \pi \cdot \sigma \tag{5}$$

In a single crystal semiconductor material, the relationship between electric field  $E$  and electric current density  $J$  is given as [29].

$$\begin{bmatrix} E_x \\ E_y \\ E_z \end{bmatrix} = \begin{bmatrix} \rho_{xx} & \rho_{xy} & \rho_{xz} \\ \rho_{xy} & \rho_{yy} & \rho_{yz} \\ \rho_{xz} & \rho_{yz} & \rho_{zz} \end{bmatrix} \begin{bmatrix} J_x \\ J_y \\ J_z \end{bmatrix} \tag{6}$$

The change in electrical resistance  $R$  in SiC is given as follows:

$$\frac{\Delta R}{R} = \frac{\Delta\rho}{\rho} = \pi_l \sigma_l + \pi_t \sigma_t + \pi_s \sigma_s \tag{7}$$

where  $\sigma_l, \sigma_t, \sigma_s$  are the longitudinal, transverse and shear stress respectively, and  $\pi_l, \pi_t, \pi_s$  are the longitudinal piezoresistive

**Table 1** Design parameters for SiC MEMS pressure sensor

Component	Mechanical dimension ( $\mu\text{m}$ )	Element thickness ( $\mu\text{m}$ )
SiC Diaphragm	1500×1500	50
SiC Polytype Piezoresistors	10(W) × 400(L)	1
Interconnector	10(W)	1
Metal Pads	160(W) × 160(L)	1

coefficient and transverse piezoresistive coefficient respectively. The  $\pi_l$ ,  $\pi_t$ ,  $\pi_s$  can be represented as  $\pi_{11}$ ,  $\pi_{12}$ ,  $\pi_{44}$  as the fundamental piezoresistive coefficient on the principal axis. Table 2 shows the piezoresistive coefficients for 3C, 4H and 6H-SiC. It is obvious that 3C-SiC offers the highest piezoresistive coefficient as compared to other hexagonal polytypes. These values are used in the piezoresistive simulation to compare the sensor sensitivity of these polytypes.

The piezoresistors are arranged on the front side of the SiC diaphragm and configured as a Wheatstone full bridge. The electrical output voltage proportional to the pressure can be represented using the following Eq. (8):

$$V_o = \frac{0.3078}{2} (\pi_l - \pi_t)(1 - \nu) \cdot \left(\frac{a}{h}\right)^2 \cdot P \cdot V_s \quad (8)$$

where  $V_o$  represents the output voltage and  $V_s$  as the bias voltage for the operation of the pressure sensor.

The Wheatstone bridge circuit, an ultra sensitive and precise technique, is considered to measure the changes in electrical resistance in voltage mode. In the presence of the external pressure, there is a change in the bridge output voltage and it is perfectly balanced under the condition when all the piezoresistors viz.  $R_1 = R_2 = R_3 = R_4$  and therefore a small change in the resistance can be detected and measured. In addition, a change in the temperature will affect all the resistors equally, cancelling each other and reflecting zero change in the output voltage. Thus if the resistance changes with temperature then it is the same amount for all piezoresistors and the bridge is balanced perfectly.

**Table 2** The piezoresistive coefficient for SiC polytypes

Polytype	Piezoresistive coefficient in $10^{-5} \text{ 1/MPa}$	Reference
3C-SiC	$\pi_{11} = 1.5$ , $\pi_{12} = -1.4$ and $\pi_{44} = 18.1$	[4]
4H-SiC	$\pi_{11} = 6.43$ , $\pi_{12} = -5.12$ and $\pi_{44} = 0$	[16]
6H-SiC	$\pi_{11} = 6.53$ , $\pi_{12} = -4.7^*$ and $\pi_{44} = 0$	[30]

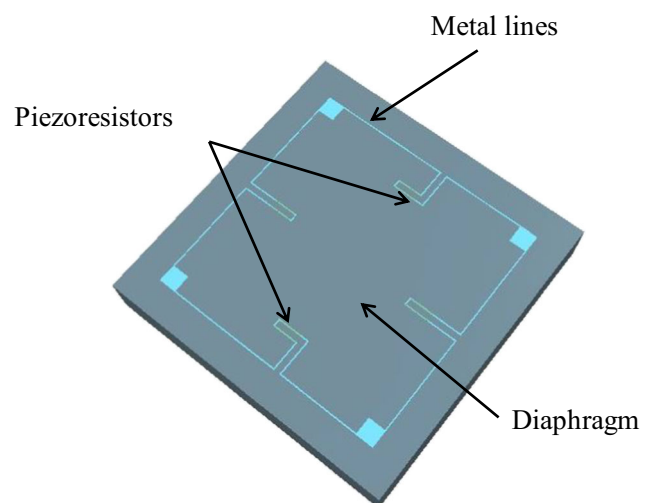
\*Assumption for simulation work due to non-availability of data

The pressure sensor sensitivity is defined as a change in output voltage per unit change in applied pressure and it can be expressed as Eq. (9):

$$S = \frac{\Delta V_o}{\Delta P \cdot V_s} = \frac{\Delta R}{\Delta P \cdot R} \quad (9)$$

### 3 Sensor Architecture

The pressure sensor consists of two key elements: Square flat thin SiC diaphragm and  $p$ -type piezoresistors. The square diaphragm of size of 1500  $\mu\text{m}$  sidelength and thickness in the range of 30 to 70  $\mu\text{m}$ . This diaphragm is supported by 750  $\mu\text{m}$  wide structure underside of the surface around the diaphragm edges. The split piezoresistors are placed in the centre of the edges of all four side of the diaphragm as shown in Fig. 2 to obtain the maximum mechanical sensitivity. The  $p$ -type piezoresistors are doped with density in the range of  $10^{14}$  to  $10^{19} \text{ cm}^{-3}$  and thickness 1  $\mu\text{m}$ . All the piezoresistors are interconnected using metal lines in Wheatstone bridge configuration.

**Fig. 2** Schematic of SiC split piezoresistors placement in Wheatstone bridge configuration on the SiC diaphragm

### 3.1 Sensor Simulation with SiC Polytypes

The pressure sensor simulation work is carried out by using commercially available MEMS device simulation software for different design parameters such as pressure range, diaphragm thickness, resistor thickness and SiC polytypes as different sensing materials to calculate the mechanical stress, deflection and sensor sensitivity.

To optimize the size of the flexible diaphragm for the operating pressure range, the diaphragm was designed using device simulation software. The diaphragm thickness is a crucial factor to determine the operating range of the sensor. To determine the optimum thickness of the square diaphragm of side length of 1500 μm, FEM simulation was executed by varying the operating pressure range and mechanical stress induced in the diaphragm. The mechanical simulation was executed by considering the diaphragm thickness in the range of 30 to 70 μm and simulation results are obtained by varying the pressure in 0 to 8 MPa range as depicted in Fig. 3. It is obvious from Fig. 3 that mechanical stress generated due to pressure increases linearly by varying the pressure for all the considered thickness of the diaphragm. To optimize the diaphragm thickness, the mechanical stress with respect to thickness at 8 MPa, FEM simulation is analyzed for 30 to 70 μm range. The response curve Fig. 3 shows that as the diaphragm thickness increases the stress magnitude gradually decreases. To achieve the higher mechanical sensitivity for the sensor higher stress plays a significant role but at the same stress must be well below the yield strength of the material i.e. 21 GPa. Thus the diaphragm thickness is decided at 50 μm by considering the safety margin of yield stress well below one fifth of the yield strength to design the pressure sensor.

To know the stress profile at the surface of the diaphragm further stress analysis was performed. Figure 4 shows the

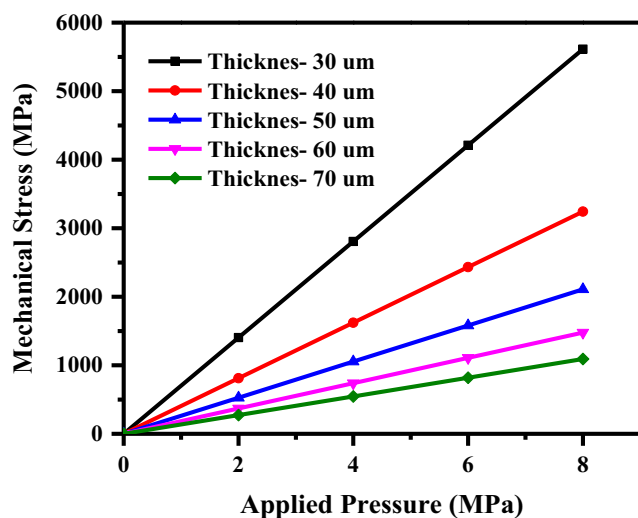


Fig. 3 Diaphragm thickness effect on deflection under the influence of varying pressure

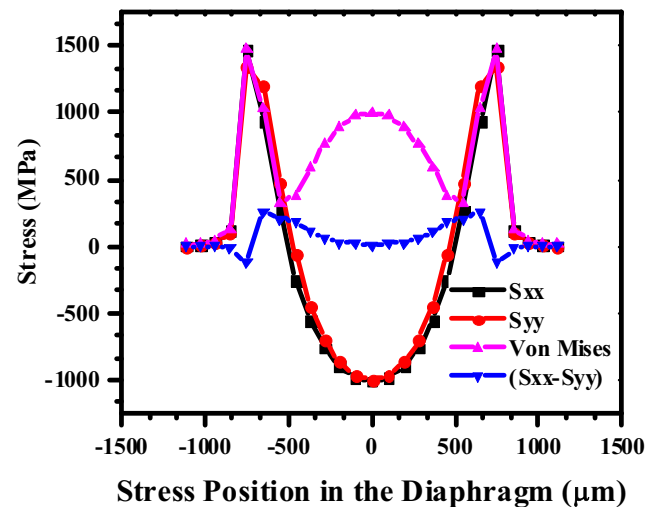


Fig. 4 Stress components of Sxx, Syy, Von mises and (Sxx-yy) profile under the influence of pressure at full load

mechanical stress components i.e.  $S_{xx}$  and  $S_{yy}$  in the longitudinal directions, and the same components are transverse directions as well due to square shape geometry. The difference between the stress components ( $S_{xx}$  and  $S_{yy}$ ) is significantly less as shown in Fig. 4 with a flat line around the central zone of the diaphragm and maximum value along the central edges of the diaphragm. In addition, a contour plot of the Von Mises stress produced in the diaphragm under the uniform pressure is also depicted in Fig. 4. The plot indicates that the piezoresistors can be placed along the centre of the edges. The other important information is that there is a deformation of diaphragm deflection in the presence of the pressure. Thus, it is decided to place the piezoresistors along the centre of the edges in the split form where the diaphragm offers maximum stress which is very essential to change the resistance of all the piezoresistors equally.

To obtain the linear performance of the pressure sensor, the other factor is the diaphragm deflection. As discussed in section 3.1, the diaphragm deflection is more linear when it deflects less as compared to its thickness. Figure 5 shows the distribution of deflection on the SiC diaphragm at full load which is significantly less as compared to the thickness of the diaphragm to assist in obtaining the linear output voltage due to linearly varying pressure. The maximum deflection is 10.5 μm as compared to the thickness of the diaphragm. Thus diaphragm thickness at 50 μm is more favourable by considering the mechanical stress and its deflection under the measured pressure range.

### 4 Results and Discussion

To understand the effect of SiC polytypes on sensor sensitivity, the effect of different design parameters like diaphragm thickness, pressure, power supply voltage, resistor thickness



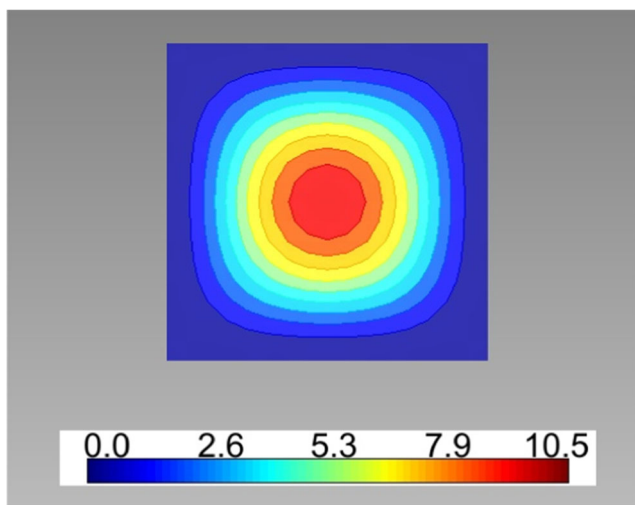


Fig. 5 Diaphragm deflection under the influence of pressure at full load

and resistivity are considered to execute the simulation using device simulation software.

### 4.1 Supply Voltage

The piezoresistors arranged in a Wheatstone bridge configuration are biased by applying the bias voltage. In the absence of external pressure, all the piezoresistors are perfectly balanced and ideally offer zero output voltage. In the presence of external pressure, the piezoresistors imbalance and exhibit change in the electrical resistance and in turn produces the output voltage. The sensor response at 8 MPa by varying the biasing voltage from 1 to 5 V as shown in Fig. 6. It is obvious from Eq. (5) as the stress (i.e. pressure) changes the material resistivity which in turn change in the output voltage showing a linear change in the output voltage with the change in bias voltage applied to the bridge and it is uniformly true for

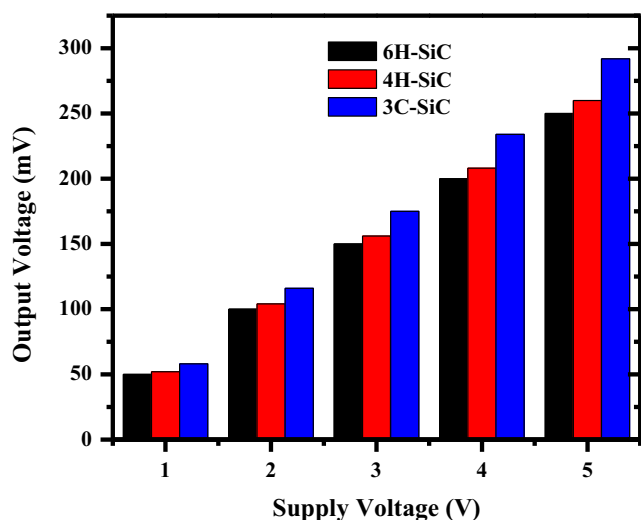


Fig. 6 Output voltage variation as a function of input bias voltage at full load

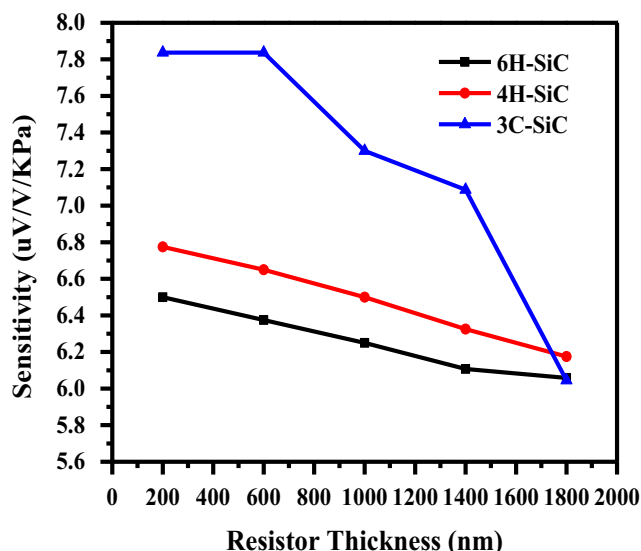


Fig. 8 Comparison of SiC polytype piezoresistors thickness effect on sensor sensitivity at full load

all the semiconductor materials. Hence, all the SiC polytypes also show linear behaviour as the bias voltage is varied. It is concluded that for a fixed pressure for the same diaphragm thickness, same size, the output voltage increases linearly with the input supply voltage. All the three SiC polytypes show the linear behaviour as given by Eq. (8) and 3C-SiC generates higher output voltage as compares to the other SiC polytypes (Fig. 6).

### 4.2 Doping Concentration

Doping concentration is another important designing parameter which affects the sensitivity of the pressure sensor. In this simulation work, to investigate the effect on all the *p*-type

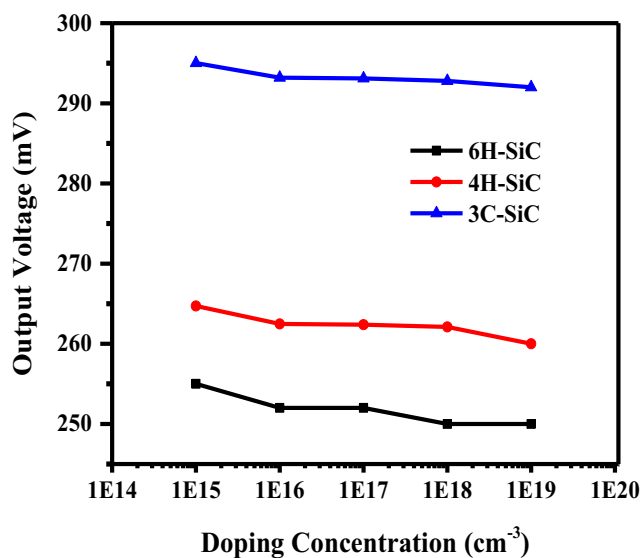


Fig. 7 Magnitude of output voltage variation as a function of doping concentration at full load

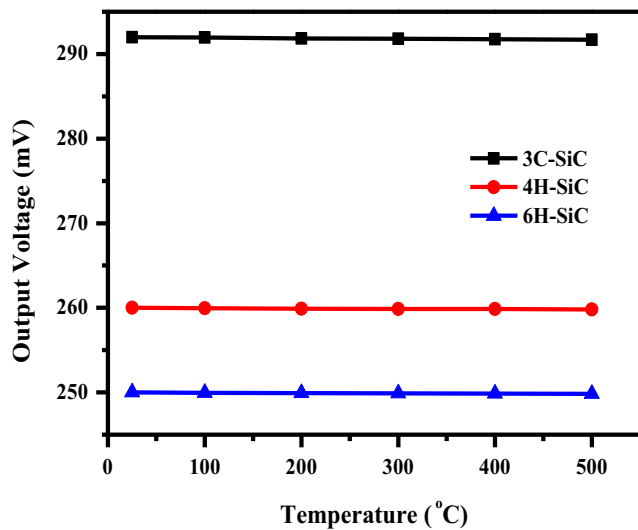


Fig. 9 Full scale output voltage as a function of temperature for sample with high doping concentration of  $10^{19} \text{ cm}^{-3}$

piezoresistors were doped in between  $10^{14}$  to  $10^{19} \text{ cm}^{-3}$  range by considering the resistor thickness at  $1 \mu\text{m}$ . The metal line connects all the piezoresistors in Wheatstone bridge configuration and piezoresistive coefficients of metal were considered at zero so that they can not affect the output voltage. The doping concentration variation effect on sensor sensitivity is shown in Fig. 7 under the influence of 8 MPa and operating voltage at 5 Vdc. The 3C-SiC offers higher mobility over 4H- and 6H-SiC [21, 30] and as the doping concentration increases, the mobility decreases which in turn gradually decrease the gauge factor hence output voltage as well [31]. The higher output voltage shown by 3C-SiC is due to higher piezoresistive coefficients. Thus, doping concentration affects the performance of the pressure sensor and in turn, degrades the sensitivity of the sensor.

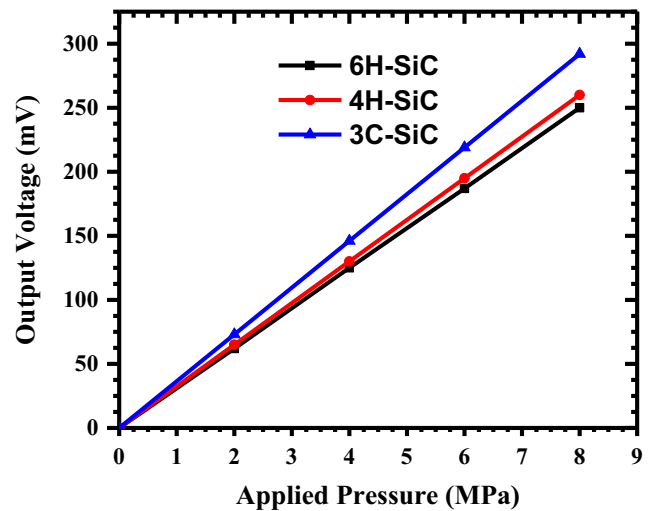


Fig. 10 Response curve between varying applied pressure and output voltage signal

### 4.3 Piezoresistor Thickness

The piezoresistor thickness is another crucial parameter which affects the sensitivity of the pressure sensor. The maximum stress due to external pressure is generated in the middle zone of the side length diaphragm as depicted in Fig. 4. The piezoresistors arranged in bridge configuration at the front side of the diaphragm to experience the maximum change in the stress. To further maximize the change in the electrical resistance due to stress, all the piezoresistors are distributed in the split form on the surface of the diaphragm as shown in Fig. 2. To understand the SiC resistors thickness effect on sensitivity of pressure sensor, piezoresistive simulation is executed for all polytypes of SiC by keeping the constant pressure at 8 MPa and the simulation results are illustrated in Fig. 8. It is the results shows as the thickness of the

Table 3 Comparative analysis of sensing parameters for SiC piezoresistive MEMS pressure sensor

SiC Resistor	Diaphragm Material	Diaphragm Size (mm <sup>2</sup> )	Diaphragm Thickness (μm)	Sensitivity (μV/V/KPa) at RT	Pressure (MPa)	Bias Voltage (V)	References
<b>3C-SiC</b>	<b>Bulk SiC</b>	<b>1.5×1.5</b>	<b>50</b>	<b>7.3</b>	<b>8</b>	<b>5</b>	<b>Present work</b>
3C—SiC	SOI	ϕ 3.3	100	20	0.5	5	[32]
3C—SiC	Si	0.75×0.75	150	14.73	0.5	10	[33]
<b>4H-SiC</b>	<b>Bulk SiC</b>	<b>1.5×1.5</b>	<b>50</b>	<b>6.5</b>	<b>8</b>	<b>5</b>	<b>Present work</b>
4H-SiC	Bulk SiC	ϕ 1	50	2.5	1.38	10	[34]
4H-SiC	Bulk SiC	ϕ 1	50	2.68	6	1	[35]
<b>6H-SiC</b>	<b>Bulk SiC</b>	<b>1.5×1.5</b>	<b>50</b>	<b>6.25</b>	<b>8</b>	<b>5</b>	<b>Present work</b>
6H-SiC	Bulk SiC	ϕ 1.48	50	1.2	6.9	5	[36]
6H-SiC*	Bulk SiC	NA	NA	3.3 μV/KPa	30	1 mA	[37]

\*NA- Not Available

piezoresistors increases, the hexagonal type SiC resistor shows the linear drop in the sensitivity of the pressure sensor. However, 3C-SiC resistor based pressure response shows a drastic drop in the sensitivity. The anisotropy of piezoresistive effect in 3C-SiC is the probable reason behind the drastic drop in the sensitivity of 3C-SiC. On the other hand, hexagonal polytypes exhibit isotropic piezoresistance [16].

#### 4.4 Temperature Effect

The influence of temperature on the pressure sensor is the other important parameter to investigate. The thermal stability of the pressure sensor is very much demanded for high temperature applications. To minimize the temperature effect, the mobility of the SiC resistors can be optimized. The high doping concentration i.e.  $\sim 10^{19} \text{ cm}^{-3}$  can minimize temperature effect on the sensor. The temperature effect on pressure sensors made of different polytypes is depicted in Fig. 9. At this level the hole mobility saturates and more limited by phonon scattering showing almost constant output voltage up to 500 °C.

#### 4.5 Pressure Response

The effect of applied pressure on electrical output voltage for different SiC polytypes based piezoresistive MEMS pressure sensor for 1  $\mu\text{m}$  thickness of the SiC diaphragm is shown in Fig. 10. It shows that the output voltage increases linearly as the applied pressure increases for all the SiC polytypes. The comparison of sensing parameters with other reported works has been shown in Table 3. The 3C-SiC comparative study shows that the 3C-SiC based piezoresistive pressure sensors fabricated on Si are included for the comparison because of the non-availability of sensor data for 3C-SiC grown on SiC diaphragm, as discussed earlier. The 3C-SiC piezoresistive pressure sensor offers higher sensitivity for  $\beta$ -SiC polytypes. Whereas between 4H-SiC and 6H-SiC polytypes, piezoresistive pressure sensor using the former offers higher sensitivity.

### 5 Conclusion

In the present study, SiC MEMS pressure sensor employing the *p*-type piezoresistors on a thin flat SiC diaphragm is proposed and its mechanical dimensions are optimized using device simulation software. The pressure sensor has been mathematically analysed to calculate the mechanical stress and deflection of the diaphragm by applying the uniform pressure up to 8 MPa and is optimized for the sensor performance. The effect of mechanical stress is studied on piezoresistive element made of different type of SiC polytypes at a given pressure for similar square geometry. The sensor sensitivity of 7.3, 6.5,

and 6.25  $\mu\text{V/V/KPa}$  for the 3C-SiC, 4H-SiC and 6H-SiC, respectively for 1  $\mu\text{m}$  thick SiC diaphragm were obtained under the influence of 8 MPa pressure. Temperature dependent output voltage in heavily doped polytypes is observed to be constant as it is mostly limited by phonon scattering in the lattice. The pressure sensor made using 3C-SiC resistors offers the highest sensitivity whereas 6H-SiC resistors offer the lowest sensitivity. This work suggests that 4H-SiC polytype, having isotropic piezoresistive coefficients and significant sensitivity, is more suitable for all practical purpose to obtain the high sensitive MEMS piezoresistive pressure sensor.

**Acknowledgements** Authors are grateful to all the scientific and technical staff of Electronics & Instrumentation Group to execute the work and allowed to use the facilities.

**Authors' Contributions** All authors discussed the content of the article, based on their domain expertise on the subjects presented. M. K. Patankar and M. Kasinathan prepare and run the simulation work. R. P. Behera developed the idea. S. Dhara and T. Jayanthi supervised the study and discussed the results, proofread the manuscript, and confirmed its findings. All authors read and approved the final manuscript.

**Data Availability** All data generated or analyzed during this study are included in this article.

**Declarations** Authors followed the ethical standards.

**Consent to Participate** Not applicable.

**Consent for Publication** This manuscript does not contain any individual person's data in any form.

**Conflict of Interests** The authors declare that they have no conflict of interests (financial and non-financial).

### References

1. Muller G, Krotz G, Niemann E (1994) SiC for sensors and high temperature electronics. *Sensors Actuators A* 43:259–268
2. Tilak V, Matocha K, Sandvik P (2006) Novel GaN and SiC based gas sensors. *phys stat sol* 3:548–553
3. Crnjac A, Skukan N, Provatas G, Mauricio R-R, Pomorski M, Jaksic M (2020) Electronic properties of a synthetic single crystal diamond exposed to high temperature and high radiation. *Materials* 13(11):2473
4. Wijesundara MBJ, Azevedo RG (2011) Silicon carbide microsystems for harsh environments. Springer, London
5. Wright NG, Horsfall AB, Vassilevski K (2008) Prospects for SiC electronics and sensors. *Mater Today* 11:16–21
6. Senesky DG, Jamshidi B, Cheng KB, Pisano AP (2009) Harsh environment silicon carbide sensors for health and performance monitoring of aerospace systems: a review. *IEEE Sensors J* 9: 1472–1478
7. Ruddy FH, Dulloo AR, Seidel JG, Hantz FW, Grobmyer LR (2002) Nuclear reactor power monitoring using silicon carbide semiconductor radiation detectors. *Nucl Technol* 140:198–208



8. Phan H-P, Nguyen T-K, Dinh T, Qamar A, Iacopi A, Lu J, Dao DV, Mina R-Z, Nguyen N-T (2019) Wireless battery free SiC sensors operating in harsh environments using resonant inductive coupling. *IEEE Electron Device Lett* 40:609–612
9. Azevedo R, Zhang J, Jones D, Myers D, Jog AV, Jamshidi B, Wijesundara M, Maboudian R, Pisano AP (2007) Silicon carbide coated MEMS strain sensor for harsh environment applications. *Proc IEEE Int Conf on Micro Electro Mechanical Systems (MEMS)*, Technical Digest 643–646
10. Muranaka T, Kikchi Y, Yoshizawa T, Shirakawa N, Akimitsu J (2008) Superconductivity in carrier-doped silicon carbide. *Sci Technol Adv Mater* 9:044204
11. Park CH, Cheong B-H, Lee K-H, Chang KJ (1994) Structural and electronic properties of cubic 2H, 4H, and 6H-SiC. *Phys Rev B* 49(7):4485–4493
12. Zetterling C-M (2002) *Process Technology for Silicon Carbide Devices*. INSPEC, Salford
13. Shi Y, Jokubavicius V, Hojer P, Ivanov IG, Yazdi G, Yakimova R, Syvajarvi M, Sun JW (2019) A comparative study of high-quality C-face and Si-face 3C-SiC(1 1 1) grown on off-oriented 4H-SiC substrates. *J Phys D Appl Phys* 52:345103
14. LaVia F, Severino A, Anzalone R, Bongiorno C, Litrico G, Mauceri M, Schoeler M, Schuh P, Wellmann P (2018) From thin film to bulk 3C-SiC growth: understanding the mechanism of defects reduction. *Mater Sci Semicond Process* 78:57–68
15. Phan H-P, Dao DV, Tanner P, Wang L, Nguyen N-T, Zhu Y, Dimitrijević S (2014) Fundamental piezoresistive coefficients of p-type single crystalline 3C-SiC. *Appl Phys Lett* 104:111905
16. Nguyen T-K, Phan H-P, Toan D, Toriyama T, Nakamura K, ARM F, Nguyen N-T, Dao DV (2018) Isotropic piezoresistance of p-type 4H-SiC in (0001) plane. *Appl Phys Lett* 113:012104
17. Barlian AA, Park W-T, Mallon JR, Rastegar AJ, Pruitt BL (2009) Review:semiconductor piezoresistance for microsystems. *Proc IEEE Inst Electr Electron Eng* 97(3):513–552
18. Stampfer C, Heldling T, Obergfell D, Schoberle B, Tripp MK, Jungen A, Roath S, Bright VM, Hierold C (2006) Fabrication of single-walled carbon-nanotube-based pressure sensors. *Nano Lett* 6(2):233–237
19. Neuzil P, Wong CC, Reboud J (2010) Electrically controlled giant piezoresistance in silicon nanowires. *Nano Lett* 10:1248–1252
20. Janssens SD, Drijkoningen S, Haenen K (2014) Ultra-thin nanocrystalline diamond membranes as pressure sensors for harsh environments. *Appl Phys Lett* 104:073107
21. Phan H-P, Dao DV, Nakamura K, Dimitrijević S, Nguyen N-T (2015) The piezoresistive effect of SiC for MEMS sensors at high temperatures: A Review. *J Microelectromech Syst* 24(6):1663–1677
22. Wu C-H, Stefanescu S, Kuo H-I, Zorman CA, Mehregany M (2001) Fabrication and testing of single crystalline 3C-SiC piezoresistive pressure sensors. *Transducers' 01 Eurosensors XV*. Springer, Berlin, pp 514–517
23. SiC substrate provider (2020) <https://www.wolfspeed.com>. Accessed on 20 Oct 2020
24. Henry A, Xun L, Jacodson H (2013) 3C-SiC heteroepitaxy on hexagonal SiC substrate. *Mater Sci Forum* 740:257–262
25. Lebedev AA, Lebedev SP, Davydov V Yu, Novikov SN, Makarov Yu N (2016) Growth and investigation SiC based heterostructures. 15<sup>th</sup> Biennial Baltic Electronics Con, Tallinn, Estonia <https://doi.org/10.1109/BEC.2016.7743717>
26. Jokubavicius V, Yazdi GR, Liljedah R, Ivanov IG, Sun J, Xinyu L et al (2015) Single domain 3C-SiC growth on off-oriented 4H-SiC substrates. *Cryst Growth Des* 15:2940–2947
27. Tai-Ran H (2008) *MEMS and microsystems: design manufacture and Nanoscale engineering*. Wiley, Hoboken
28. Mario DG (1982) *Flat and corrugated diaphragm design handbook*. CRC Press, Boca Raton
29. Nguyen TK (2018) *Piezoresistive effect in 4H silicon carbide towards mechanical sensing in harsh environments* PhD Griffith University
30. Okojie RS, Ned AA, Kurtz AD, Carr WN (1998) Characterization of highly doped n- and p-type 6H-SiC piezoresistors. *IEEE Trans Electron Devices* 45(4):785–790
31. Takaya S, Takahashi N, Nakano N (2020) The piezoresistive mobility modeling for cubic and hexagonal silicon carbide crystals. *J Appl Phys* 127:245113
32. Ziermann R, Berg JV, Obermeier E, Wischmeyer F, Niemann E, Moller H, Eickhoff M, Krotz G (1999) High temperature piezoresistive  $\beta$ -SiC-on-SOI pressure sensor with on chip SiC thermistor. *Mater Sci Eng* 61-62:576–578
33. Wu C-H, Zorman CA, Mehran M (2006) Fabrication and testing of bulk micromachined silicon carbide piezoresistive pressure sensors for high temperature applications. *IEEE Sensors J* 6:316–324
34. Okojie RS, Lukco D, Nguyen V, Savrun E (2015) 4H-SiC piezoresistive pressure sensors at 800 °C with observed sensitivity recovery. *IEEE Electron Device Lett* 36(2):174–176
35. Akiyama T, Briand D, Rooij NF (2011) Piezoresistive n-type 4H-SiC pressure sensor with membrane formed by mechanical milling. *Proc IEEE Sens:222–225* <https://doi.org/10.1109/ICSENS.2011.6126936>
36. Okojie RS, Ned AA, Kurtz AD (1998) Operation of  $\alpha$ (6H)-SiC pressure sensor at 500°C. *Sensors Actuators A* 66:200–204
37. Wiczorek G, Schellin B, Obermeier E, Fagnani G, Drera L (2007) SiC based pressure sensor for high-temperature environments. *Proc IEEE Sens:748–751* <https://doi.org/10.1109/ICSENS.2007.4388508>

**Publisher's Note** Springer Nature remains neutral with regard to jurisdictional claims in published maps and institutional affiliations.